

9. SITE 1015¹

Shipboard Scientific Party²

HOLE 1015A

Date occupied: 12 May 1996
Date departed: 12 May 1996
Time on hole: 14 hr
Position: 33°42.925'N, 118°49.185'W
Drill pipe measurement from rig floor to seafloor (m): 911.9
Distance between rig floor and sea level (m): 11.1
Water depth (drill pipe measurement from sea level, m): 900.8
Total depth (from rig floor, m): 1061.4
Penetration (m): 149.5
Number of cores (including cores having no recovery): 16
Total length of cored section (m): 149.5
Total core recovered (m): 139.1
Core recovery (%): 93.0
Oldest sediment cored:
Depth (mbsf): 149.5
Nature: Quartz feldspar silty sand
Age: Quaternary

HOLE 1015B

Date occupied: 12 May 1996
Date departed: 13 May 1996
Time on hole: 09 hr, 45 min
Position: 33°42.922'N, 118°49.118'W
Drill pipe measurement from rig floor to seafloor (m): 912.1
Distance between rig floor and sea level (m): 11.1
Water depth (drill pipe measurement from sea level, m): 901.0
Total depth (from rig floor, m): 1008.9
Penetration (m): 97.8
Number of cores (including cores having no recovery): 12
Total length of cored section (m): 97.8
Total core recovered (m): 81.4
Core recovery (%): 83.1%
Oldest sediment cored:
Depth (mbsf): 97.8
Nature: Silty clay, clay with nannofossils and silt
Age: Quaternary

Principal results: Site 1015 is located in the Santa Monica Basin at a water depth of 901 mbsl. It is the only Leg 167 site located within an inner borderland basin. This basin is known to have had anoxic periods because the source of deep water is very near the oxygen minimum. Distal turbidites from the Hueneme fan extend to Site 1015. The primary objective for drilling here was to sample a very high-resolution sediment section for comparison with ODP Site 893 in the Santa Barbara Basin. Hemipelagic sections between turbidites should be sufficiently large to study upper Pleistocene and Holocene paleoceanographic processes. The site should also prove useful for sedimentological study of turbidite deposition and the development of Hueneme Fan.

Two holes were cored with the APC at Site 1015 to a depth of 149.5 and 97.8 mbsf, respectively. Detailed comparisons of the two holes between the magnetic susceptibility and the GRAPE density generated on the MST and high-resolution color reflectance measured with the Oregon State University system, demonstrated complete recovery of the sedimentary sequence down to 36 mbsf. The existence of gas voids, turbidites, and coring disturbances below that depth precluded any further continuous interhole correlations.

The sedimentary sequence consists of a 150-m-thick interval of upper Quaternary sediments. Sediments form one lithostratigraphic unit that is characterized by decimeter- to meter-scale rhythmic repetition of graded sand with sharp basal contacts, homogeneous non-bioturbated silts and clays, and laminated and possibly bioturbated nannofossil clay. The sharp basal contacts, normal grading, and well-sorted nature of the sand strongly suggest turbidite deposition. Four intervals containing laminated nannofossil clay are present within the upper 90 m of the sequence. These are interrupted by intervals with homogeneous, possibly bioturbated nannofossil clay. The repetition of laminated and bioturbated(?) intervals may represent millennial-scale oscillation of bottom-water oxygenation levels during the latest Pleistocene and Holocene similar to that from the adjacent Santa Barbara Basin (ODP Site 893).

Biostratigraphic age control was provided by calcareous nannofossils and planktonic foraminifers that indicate a latest Quaternary age, younger than 60 ka. Sand layers in the sequence are barren of microfossils except for very rare, moderately well-preserved calcareous nannofossils in some intervals. Hemipelagic sediments contain well-preserved planktonic and benthic foraminifers and calcareous nannofossils. Radiolarians and diatoms are essentially absent, except for reworked Miocene taxa.

Changes in planktonic foraminifer assemblages in this sequence exhibit evidence of Quaternary oscillations between glacial and interglacial conditions. The Holocene is well marked by distinct planktonic foraminifer assemblages. Planktonic and benthic foraminifer assemblages suggest that the glacial-interglacial episodes are associated with changes in circulation of upper intermediate waters, which influenced oxygen levels in the basins of the California Borderland.

Gas voids, turbidites, and coring disturbances precluded the measurement of most physical properties. A paleomagnetic reversal stratigraphy could not be obtained because of the young age of the sediment and the coring disturbances.

Carbonate values range between 2 and 7 wt%. Lowest values occur in the turbidites. The organic carbon record shows hemipelagic background values of ~1–1.5 wt%, with <0.5 wt% in the coarse-grained turbidites. Wood fragments in the sediment contribute to high values up to 2.3 wt%.

¹Lyle, M., Koizumi, I., Richter, C., et al., 1997. *Proc. ODP, Init. Repts.*, 167: College Station, TX (Ocean Drilling Program).

²Shipboard Scientific Party is given in the list preceding the Table of Contents.

Although the chemical composition of the interstitial water samples from this site indicates that organic matter diagenesis, biogenic opal dissolution, and authigenic mineral precipitation and/or ion exchange reactions are significant influences, drilling disturbance of the sediments makes distinguishing primary geochemical signals from drilling fluid contamination problematic.

BACKGROUND AND OBJECTIVES

General Description

Site 1015 is located about 30 km west of Los Angeles, California, in Santa Monica Basin. It is the only Leg 167 drill site within an inner borderland basin (Fig. 1). Water depth at the drill site is shallow (901 mbsl), and the sill depth for waters entering Santa Monica Basin is 737 mbsl (Emery, 1960). Deep water entering the basin is at the end of a flow path that began at Animal Basin (Site 1011). The source of deep water is also very near the oxygen minimum, so that the basin periodically becomes anoxic (D. Gorsline, pers. comm., 1995) The site is located near the center of the basin because the Holocene cycles of anoxic events seem to expand outward from the center.

Santa Monica Basin is occupied in its northern end by the Hueneme Fan, which is formed at the base of Hueneme and Mugu Submarine Canyons near Oxnard, California. Distal turbidites from the fan extend to Site 1015, with numerous turbidites throughout the recovered section. The site has the highest sedimentation rate of the Leg 167 drill sites, and the age for the base of drilling is late Quaternary.

The site was surveyed in detail with the *Maurice Ewing* on cruise EW9504 in 1995 (Lyle et al., 1995a, 1995b; Fig. 2). The basin fill is extremely flat, changing less than 10 m over 10 km, and has high acoustic return, typical of turbidites. Individual layers can be traced up the western slope of the Santa Monica Basin, which indicates that

occasional very large turbidity flows cascaded into the basin. Depth to basement is difficult to determine beneath the drill site, but is significantly deeper than the 150 mbsf drilled.

Site Objectives

Site 1015 was drilled to sample a very high-resolution sediment section to compare with Santa Barbara Basin (ODP Site 893). While it may be possible to use the hemipelagic sections between turbidites to study late Pleistocene and Holocene paleoceanographic processes, it will be difficult to assign age control points and verify continuity of the section. The site may also prove useful for sedimentological study of turbidite deposition in Santa Monica Basin and the development of Hueneme Fan. Organic carbon diagenesis, through geochemical analyses of the solids, can be studied in a sedimentary section that has been quickly deposited and where there is likely to be a large terrigenous organic component.

OPERATIONS

Transit from Site 1014 to Site 1015

The 85.0-nmi transit from Site 1014 to Site 1015 was accomplished in 7.75 hr at an average speed of 11.0 kt. A 3.5-kHz precision depth recorder survey was performed while approaching Site 1015. The *JOIDES Resolution* arrived at Site 1015 at 0530 hr on 12 May.

Hole 1015A

Hole 1015A was spudded at 0815 hr on 12 May. APC Cores 167-1015A-1H through 16H were taken from 0 to 149.5 mbsf with 93.1%

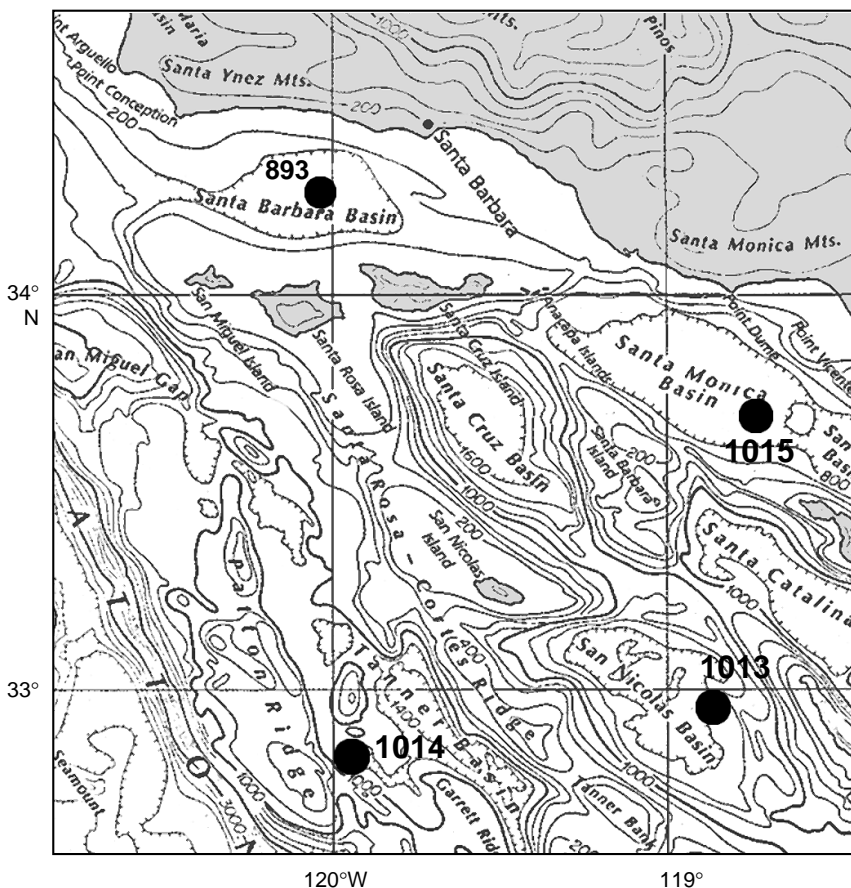


Figure 1. Location map for Site 1015, showing its position with respect to other northern California Borderland drill sites. Site 1015, in Santa Monica Basin and Site 893 (Santa Barbara Basin) are within inner Borderland basins, whereas Site 1013, in San Nicolas Basin, is in the middle Borderland belt, and Site 1014 is located in the outer Borderland.

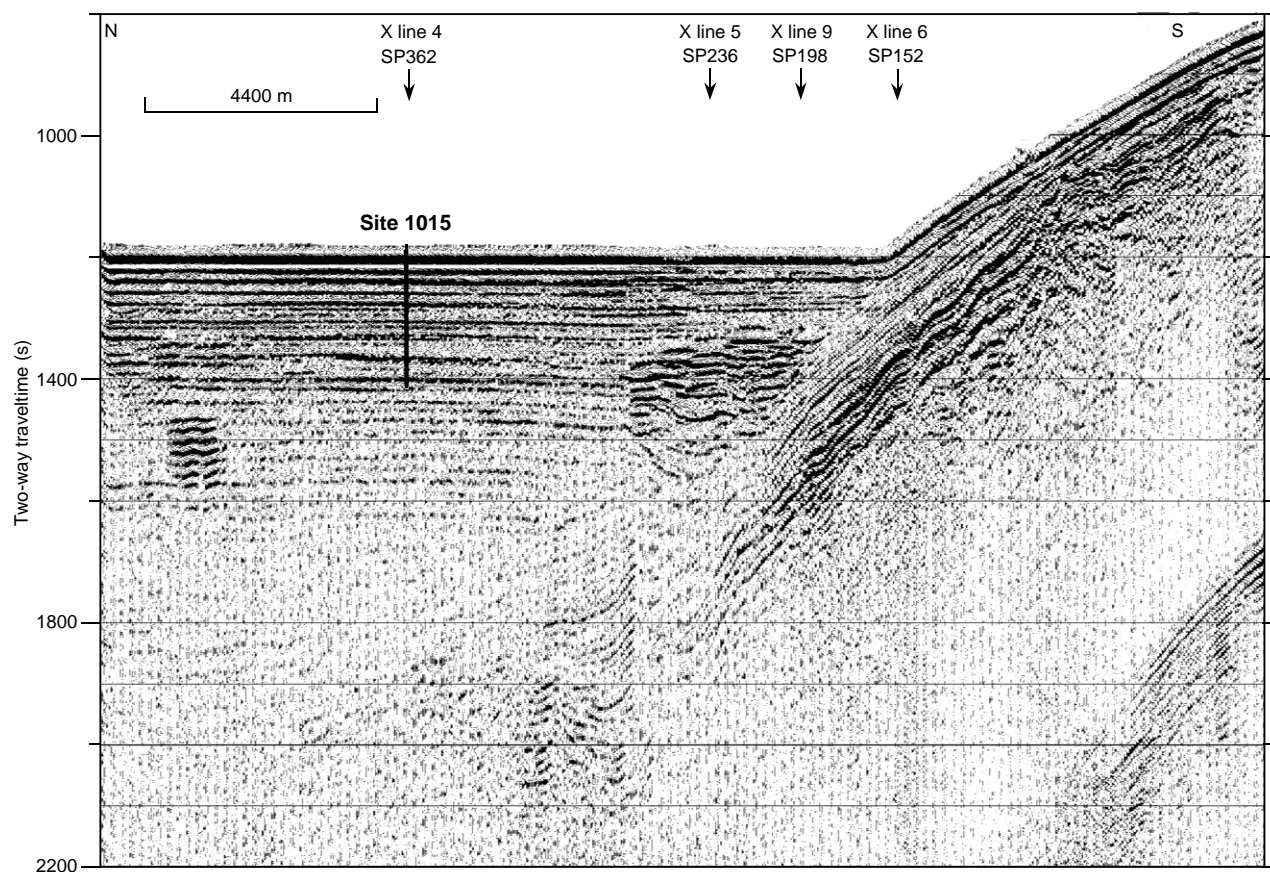


Figure 2. Seismic reflection profile through Site 1015 (Line EW9504 BA4-1; Lyle et al., 1995a, 1995b). The data are summed 4-channel data, filtered between 30 and 200 Hz, with predictive deconvolution and Stolt F-K migration applied. Santa Monica Basin is filled with a thick sequence of turbidites interlayered with more hemipelagic sediments. Site 1015 was drilled to a depth of 150 mbsf, and an upper Pleistocene sequence of sediments was recovered. On y-axis, (s) = milliseconds.

recovery (Table 1; see Table 2 on CD-ROM in the back pocket of this volume for a more detailed coring summary). Oriented cores were obtained on Cores 167-1015A-3H through 9H. An Adara temperature measurement was run on Core 4H. Further Adara measurements were canceled because of overpull and the slow APC bit advancement. The recovered core exhibited multiple turbidites, which contributed to the slow drilling conditions. The vessel was offset 100 m to the east in an attempt to find an area more conducive to APC coring.

Hole 1015B

Hole 1015B was spudded at 2000 hr on 12 May. APC Cores 167-1015B-1H through 12H were taken from 0 to 97.8 mbsf with 83.2% recovery (Table 1). The APC coring system encountered refusal in Core 12H and the hole was terminated. The drill string was tripped back to the surface and secured for the 16-hr transit to Site 1016 by 0545 hr on 13 May.

LITHOSTRATIGRAPHY

Introduction

A 149.5-m-thick, upper Quaternary sedimentary sequence was recovered at Site 1015. Sediments are dominated by decimeter- to meter-scale repetition of quartz feldspar sand and clayey silt (Fig. 3). Sand layers show sharp basal contacts and grade upwards into clayey silt, suggesting deposition by turbidity currents. Carbonaceous wood

fragments are common in the upper part of sand layers. Thin layers of (<10 cm) laminated hemipelagic nannofossil clay frequently overlie the clayey silt and in turn are overlain by sand. Volcanic glass is a locally important siliciclastic component but does not occur as discrete layers. Micrometer-size authigenic pyrite is a minor but common constituent of the sediment. The biogenic component is dominated by nannofossils with subordinate amounts of foraminifers in the hemipelagic layers but is an insignificant percentage of the clayey silt and sand layers. Siliceous microfossils such as diatoms and radiolarians are rare to absent.

The sediments were grouped into a single lithostratigraphic unit based on visual core descriptions and smear-slide estimates (Fig. 3).

Description of Unit

Unit I

Hole 1015A, intervals 167-1015A-1H-1 through 16H-CC, 0–149.50 mbsf (base of hole);

Hole 1015B, intervals 167-1015B-1H-1 through 12H-CC, 0–97.8 mbsf (base of hole).

Age: Quaternary, 0.0–0.06 Ma.

Unit I is predominantly composed of a rhythmic repetition of medium- to fine-grained quartz feldspar sand and clayey silt or silty clay with frequent intercalations of nannofossil clay to clay with nannofossils and silt. Sand and clayey silt are medium gray (N 5) to grayish black (N 3) in freshly split core surfaces, but oxidation causes the color to change quickly (<1 hour) to olive gray (5Y 5/2) to olive (5Y 4/

Table 1. Coring summary for Site 1015.

Core	Date (May 1996)	Time	Top (mbsf)	Bottom (mbsf)	Length cored (m)	Length recovered (m)	Recovery (%)
167-1015A-							
1H	12	1515	0.0	7.0	7.3	7.00	100.0
2H	12	1600	7.0	16.5	9.5	10.26	108.0
3H	12	1650	16.5	26.0	9.5	10.53	110.8
4H	12	1750	26.0	35.5	9.5	8.59	90.4
5H	12	1850	35.5	45.0	9.5	10.10	106.3
6H	12	1930	45.0	54.5	9.5	10.34	108.8
7H	12	2010	54.5	64.0	9.5	7.31	76.9
8H	12	2045	64.0	73.5	9.5	8.93	94.0
9H	12	2130	73.5	83.0	9.5	10.79	113.6
10H	12	2210	83.0	92.5	9.5	6.14	64.6
11H	12	2235	92.5	102.0	9.5	4.04	42.5
12H	12	2320	102.0	111.5	9.5	8.94	94.1
13H	12	2350	111.5	121.0	9.5	9.88	104.0
14H	13	0035	121.0	130.5	9.5	8.27	87.0
15H	13	0135	130.5	140.0	9.5	8.18	86.1
16H	13	0135	140.0	149.5	9.5	9.79	103.0
167-1015B-							
1H	13	0315	0.0	2.3	2.3	2.36	102.0
2H	13	0335	2.3	11.8	9.5	9.94	104.0
3H	13	0400	11.8	21.3	9.5	9.70	102.0
4H	13	0425	21.3	30.8	9.5	9.47	99.7
5H	13	0455	30.8	40.3	9.5	8.99	94.6
6H	13	0535	40.3	49.8	9.5	5.83	61.3
7H	13	0610	49.8	59.3	9.5	8.61	90.6
8H	13	0645	59.3	68.8	9.5	6.40	67.3
9H	13	0720	68.8	78.3	9.5	7.68	80.8
10H	13	0800	78.3	87.8	9.5	9.42	99.1
11H	13	0840	87.8	97.3	9.5	2.41	25.3
12H	13	0945	97.3	97.8	0.5	0.51	5.4

Note: Table 2, on the CD-ROM in the back pocket, this volume, is a more detailed coring summary.

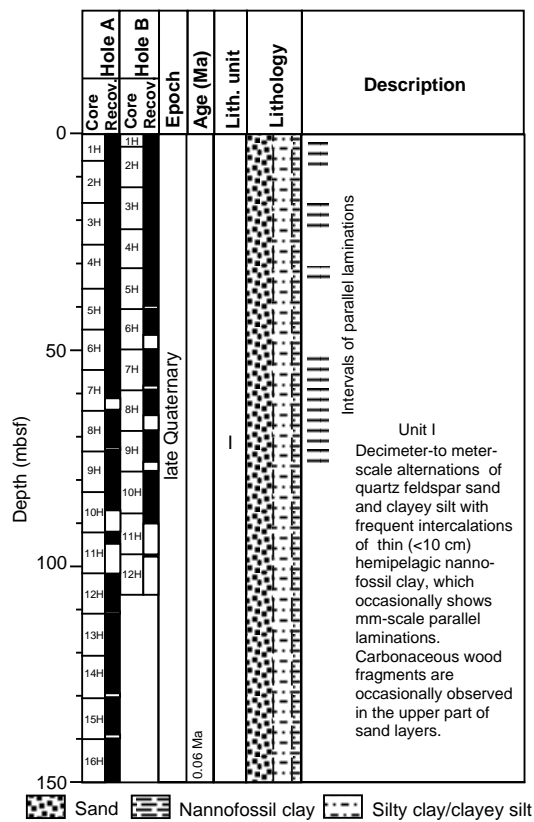


Figure 3. Site 1015 lithostratigraphic summary (0–149.50 mbsf).

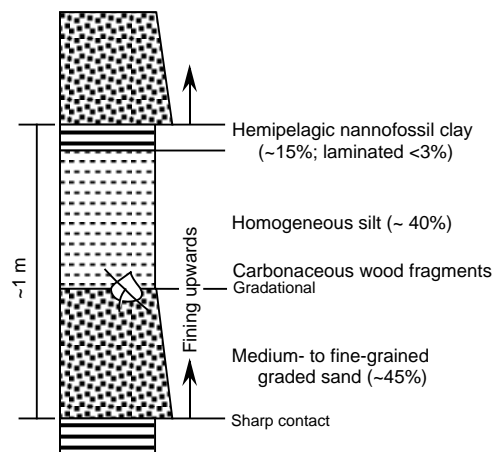


Figure 4. A schematic sketch of sand-silt-nannofossil clay alternation.

2). Nannofossil clay is olive (5Y 5/3 to 5Y 4/3) but also changes color slightly with time.

Sand layers are centimeter-scale to more than a meter thick, show sharp basal contacts with locally scoured surfaces, and normally grade upward into clayey silt (Fig. 4). They are generally structureless, although faint lamination is observable in some cases. Sand layers compose approximately 45% of the upper 50 m of the sedimentary sequence. Clayey silt or silty clay layers are a centimeter to more than a meter thick, fine upwards slightly, and are either homogeneous or show subhorizontal irregular olive (5Y 5/3) color laminations (pseudolaminae) on scraped surfaces. Composition of the pseudolaminae is similar to that of the host clayey silt; therefore, it is likely that pseudolamination is related to an oxidation reaction along fissile partings during core exposure to the atmosphere. There is no evidence of bioturbation in the clayey silt or silty clay. Carbonaceous wood fragments are occasionally found either in the uppermost part

of sand layers or the lower part of clayey silt layers. Clayey silt layers compose ~40% of the sedimentary sequence. Sands dominantly comprise quartz and feldspar with subordinate amounts of amphibole and mica. Volcanic glass is abundant locally. Sands enriched in volcanic glass also tend to be enriched in biotite and amphibole. Framboidal pyrite is a minor but common component of the silt fraction.

Centimeter- to decimeter-thick nannofossil clay to clay with nannofossils and silt generally overlies the clayey silt and forms the top part of the repetitive sequence of sedimentation (Fig. 4). This lithology contains as much as 40% nannofossils and 8% foraminifers based on smear-slide observations. Nannofossil clay occasionally shows millimeter-scale, olive (5Y 4/3) and black (N 2) parallel laminations (Fig. 5). Olive laminae tend to be slightly enriched in nannofossils, whereas black laminae are enriched in pyrite. Sequences of laminae are generally 1 cm to 3 cm thick and rarely exceed 10 cm. The base of laminated layers always has a sharp contact with underlying homogeneous clayey silt and their top contact is cut sharply by overlying sand. When nannofossil clay is not laminated, its lower boundary is generally gradational. This relationship is probably related to biomixing, although distinct burrows are not observed. Laminated layers occur in several discrete intervals: ~4 to 8 mbsf, 17 to 25 mbsf, 31 to 33 mbsf, and 50 to 75 mbsf. Nannofossil clay constitutes ~15% of the sedimentary sequence of the upper 50 m, but laminated nannofossil clay forms <3%.

A 30-cm-thick interval of disaggregated wood was recovered in Section 167-1015B-10H-3. It occurs in the uppermost part of a homogeneous clayey silt layer. Cores 167-1015A-12H to 16H are filled with soupy sand, suggesting that sand is the dominant lithology below ~100 mbsf.

Depositional Conditions

Sediments at Site 1015 are characterized by decimeter- to meter-scale rhythmic repetition of graded sand with sharp basal contacts, homogeneous non-bioturbated clayey silt to silty clay, and laminated and possibly bioturbated nannofossil clay. The sharp basal contacts, normal grading, and well-sorted nature of the sand strongly suggest turbiditic deposition. The gradational change from the underlying sand, the non-bioturbated, homogeneous appearance, combined with the slightly fining-upward nature and lack of planktonic microfossils are all consistent with the hypothesis that the clayey silt to silty clay compose the upper part of turbidite beds. The lack of sedimentary structures characteristic of classic turbidite deposits (Stow and Wetzel, 1990) does not allow confirmation of this origin. An alternative explanation for the origin of clayey silt and silty clay include flood deposits that were transported along the pycnocline created during flood events (Drake et al., 1972). In either case, sand and clayey silt layers at Site 1015 likely represent instantaneous event deposits rather than continuous background deposition. Smear-slide observations suggest at least two different sources of siliciclastics, one enriched in quartz and feldspar and the other enriched in volcanic glass, biotite, and amphiboles.

Nannofossil clay, on the other hand, seems to represent background hemipelagic deposition. The presence of millimeter-scale parallel laminations, as well as the in situ foraminifers within this lithology (see "Biostratigraphy" section, this chapter), is also consistent with a hemipelagic origin. Four intervals characterized by laminated nannofossil clay are recognized within the upper 90 m of the sequence, which are interrupted by intervals characterized by homogeneous, possibly bioturbated nannofossil clay. Since presence of lamination and bioturbation imply suboxic to anoxic and oxic bottom-water conditions, respectively (Savrda et al., 1984), repetition of these laminated and possibly bioturbated intervals may represent millennial-scale oscillation of bottom-water oxygenation levels during the latest Pleistocene and Holocene (see "Biostratigraphy" section, this chapter) similar to that of the adjacent Santa Barbara Basin (Behl and Kennett, 1996).

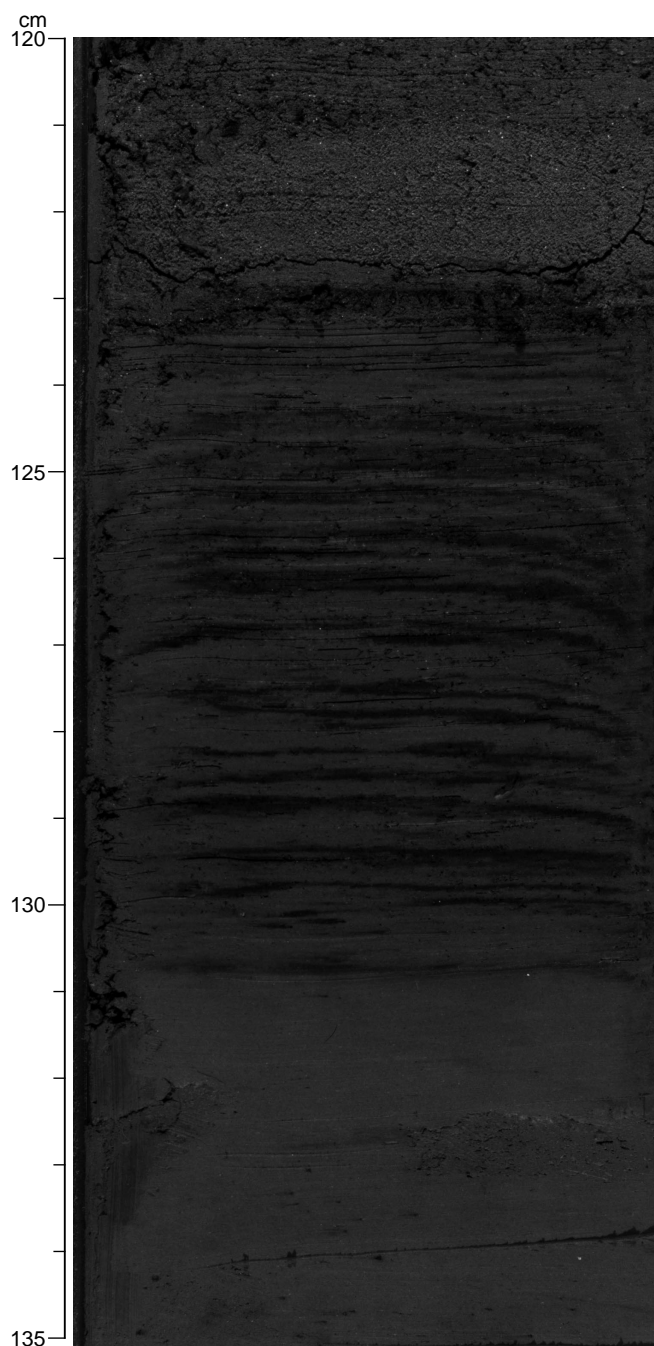


Figure 5. A close-up of laminated nannofossil clay overlying clayey silt, and in turn overlain by a sand turbidite (Sample 167-1015A-3H-6, 120–135 cm).

BIOSTRATIGRAPHY

Calcareous nannofossil and planktonic foraminifer data indicate that the 150-m sequence of turbidites and hemipelagic sediments at Site 1015 are of latest Quaternary age, younger than 60 ka. Site 1015 is represented by a single calcareous nannofossil Zone CN15, which dates the sequence as younger than 85 ka. The paleoclimatic sequence indicated by changes in planktonic foraminifers suggests that the base of the sequence is no older than 60 ka. Sand layers in the sequence are barren of microfossils except for very rare, moderately well-preserved calcareous nannofossils in some intervals. Hemipelagic sediments contain abundant to few, well-preserved planktonic foraminifers, common to abundant, well-preserved benthic foramin-

ifers, and abundant to rare, well-preserved calcareous nannofossils. Radiolarians are conspicuous only at the very top of the sequence (Sample 167-1015A-1H-CC) and are essentially absent below, except for pervasive reworked Miocene forms. Diatoms are absent throughout the sequence except for reworked Miocene taxa.

Changes in planktonic foraminifer assemblages in this sequence exhibit clear evidence of large-scale Quaternary glacial-interglacial oscillations. The Holocene is well marked by interglacial planktonic foraminifer assemblages and is ~31 m thick. Below the Holocene, planktonic foraminifers exhibit faunal variability seen during glacial isotopic Stages 2 and 3 in Santa Barbara Basin (Kennett and Venz, 1995). Planktonic foraminifer assemblages occurring at some levels during oxygen isotopic Stage 3 reflect sea-surface temperatures as intermediate between full interglacial and glacial conditions and may represent interstadial episodes. Benthic foraminifer assemblages inferred to be closely associated with very low oxygen levels in basinal waters occur together with relatively warm planktonic foraminifer assemblages. In contrast, cooler planktonic foraminifer assemblages are often associated with benthic forms indicative of more highly oxygenated bottom waters. This suggests that the glacial-interglacial episodes are associated with changes in circulation of upper intermediate waters affecting changes in oxygen levels of the basins of the California Borderlands.

Planktonic Foraminifers

Planktonic foraminifers at Site 1015 indicate a sequence ranging in age from the Holocene through latest Pleistocene oxygen isotopic Stage 3 (Table 3). The age of the base of the sequence is not yet known, but the sequence of climatic cycles suggests that it is younger than Stage 4 (60 ka). The core-catcher samples examined from Site 1015 are from two distinct sediment facies: fine sand turbidites and hemipelagic sediments. Both planktonic and benthic foraminifers are completely absent in sediments dominated by fine sands. In contrast, samples from hemipelagic layers contain abundant to few well-preserved planktonic foraminifers and common to abundant well-preserved benthic foraminifers. The great majority of planktonic foraminifers observed are in place. A small percentage of specimens are

clearly reworked from shallower depths and are poorly preserved. Changes in planktonic foraminifer assemblages in this sequence exhibit clear evidence of large-scale Quaternary glacial-interglacial oscillations.

The uppermost part of Hole 1015A (Samples 167-1015A-1H-CC to 3H-CC) and Hole 1015B (Samples 167-1015B-1H-CC to 4H-CC) contains relatively warm-water planktonic foraminifers including *Neogloboquadrina pachyderma* (dextral) and *N. dutertrei*. Below this level, the sequence contains cooler water planktonic foraminifers including *N. pachyderma* (sinistral). The base of the warm-water assemblages in the upper part of the sequence is considered to represent the base of the Holocene (~11 ka). This shows that the Holocene is ~31 m thick at Site 1015. Changes in composition of planktonic foraminifers before the Holocene reflect oscillations in climatic conditions during the last glaciation that require documentation. The inferred coldest assemblages occur between Samples 167-1015A-8H-CC and 12H-CC. There is no evidence for interglacial planktonic foraminifer assemblages near the bottom of the cored sequence that might indicate presence of the last interglacial episode (oxygen isotope Stage 5).

Benthic foraminifers occur in all hemipelagic sediment intervals in variable abundances. They are often abundant, diverse, and well preserved, and are especially well preserved in the Holocene sediments. Holocene assemblages are dominated by *Bolivina* spp., especially *B. spissa* and *B. argentea* which, in Santa Barbara Basin Site 893, are associated in abundance with laminated sediments, representing very low oxygen levels of bottom waters (Kennett, Baldauf, Lyle, et al., 1995). This also appears to be the case in Santa Monica Basin Site 1015. The preliminary evidence from Site 1015 also indicates that the benthic foraminifer assemblages inferred to be closely associated with very low oxygen levels in basinal waters are also associated with the warmest intervals based upon planktonic foraminifer assemblages. Holocene (interglacial) assemblages are dominated by *Bolivina* spp. and also include *Globobulimina*, *Rutherfordoides*, *Buliminella*, *Cassidulina*, and *Uvigerina*. Such an assemblage indicates low-oxygen bottom waters during the Holocene. In contrast, assemblages of glacial age are often dominated by *Uvigerina* and have *Oridorsalis*, *Globobulimina*, *Epistominella*, *Baggina*, *Cibicidoides*,

Table 3. Distribution and abundances of planktonic foraminifers in Hole 1015A.

Zone	Core, section, interval	Depth (mbsf)	Abundance	Preservation	<i>Neogloboquadrina dutertrei</i>	<i>Globorotalia inflata</i>	<i>Neogloboquadrina pachyderma</i> dex.	<i>Neogloboquadrina pachyderma</i> sin.	<i>Globigerina bulloides</i>	<i>Orbulina universa</i>	<i>Globigerinoides ruber</i>	<i>Globorotalia scitula</i>	<i>Globigerinita glutinata</i>	<i>Globigerina quinqueloba</i>	<i>Globorotalia truncatulinoides</i>	<i>Hasigerina aequilateralis</i>	<i>Globigerina falconensis</i>
N22/23	167-1015A-1H-CC	7.0	A	G	R		C		R	F	R						
	2H-CC	17.0	C	G	F		C		R	F							
	3H-CC	26.0	C	G	F	C	F		C	F	R				R	R	
	4H-CC	36.0	B														
	5H-CC	45.0	F	G			R	C	F					R	C		R
	6H-CC	54.0	F	G			F	F		R		R		R			
	7H-CC	64.0	F	G			C	F							C		
	8H-CC	74.0	C	G				A	C	R				R			
	9H-CC	83.0	A	G				A	A	R		R		R	A		
	10H-CC	93.0	F	G				C	A						C		
	11H-CC	102.0	A	G				A	A				R		A		
	12H-CC	112.0	A	G				A	A				R		A		
	13H-CC	121.0	B														
	14H-CC	131.0	B														
	15H-CC	140.0	C	G	R		F	C	C			R	R				
	16H-CC	150.0	F	G			F		C	F							

Note: See "Explanatory Notes" chapter for abbreviations.

Pyrgo, and other forms indicative of more oxygenated waters. Assemblages of intermediate character also occur during the glacial interval. Therefore, the late Quaternary sequence at Site 1015 suggests that the glacial-interglacial episodes are associated with changes in circulation of upper intermediate waters that affect changes in oxygen levels of the basins of the California Borderland.

Calcareous Nannofossils

The calcareous nannofossils at Site 1015 are abundant to absent and generally well preserved throughout the sequence. Holes 1015A and 1015B represent an interval spanning the latest Pleistocene to Holocene Zone CN15 (Table 4).

Nannofossil assemblages are marked by a dominance of *Emiliania huxleyi*, the presence of *Helicosphaera carteri*, and several morphotypes of *Gephyrocapsa* spp. The dominance of *E. huxleyi* indicates an age younger than 85 ka (bottom of acme of *E. huxleyi*). In addition, several specimens of *E. huxleyi* are large (4 μm), supporting this younger age.

Diatoms

Diatoms are either absent or occur only in trace amounts and are of no value for biostratigraphy at Site 1015 (Table 5). Those present are very poorly preserved. The uppermost core-catcher samples of Holes 1015A and 1015B (Samples 167-1015A-1H-CC and 167-1015B-1H-CC) contain common to few siliceous bands dislodged from the girdles of diatom cells.

COMPOSITE DEPTHS AND SEDIMENTATION RATES

Multisensor track (MST) data collected at 5-cm intervals from Holes 1015A and 1015B and color reflectance data collected at 4- to 6-cm intervals from Holes 1015A and 1015B were used to determine depth offsets in the composite section. On the composite depth scale (expressed as mcd, meters composite depth), features of the plotted MST data present in adjacent holes are aligned so that they occur at approximately the same depth. Working from the top of the sedimentary sequence, a constant was added to the mbsf (meters below sea floor) depth for each core in each hole to arrive at a mcd depth for that core. The depths offsets that compose the composite depth section are given in Table 6 (also on CD-ROM, back pocket). Continuity of the sedimentary sequence was documented for the upper 36 mcd.

Magnetic susceptibility was the primary parameter used for inter-hole correlation purposes. GRAPE bulk density and color reflectance measurements were used in a few intervals to provide additional support for composite construction. Natural gamma-ray activity measurements were made only in Hole 1015B.

The magnetic susceptibility, GRAPE bulk density, and color reflectance records for Site 1015 are shown on a composite depth scale in Figure 6. The GRAPE data were used to identify intervals of voids and highly disturbed sediments (values $<1.4 \text{ g/cm}^3$) and these intervals were culled from all the MST and color reflectance data sets. The cores from Holes 1015A and 1015B provide continuous overlap to about 36 mcd. Below 36 mcd, some cores were correlated to each other, but composite records and splices could not be constructed be-

Table 4. Distribution and abundances of calcareous nannofossils in Holes 1015A and 1015B.

Zone	Core, section, interval	Depth (mbsf)	Preservation	Abundance	<i>Emiliania huxleyi</i>	<i>Pseudoemiliania lacunosa</i>	<i>Helicosphaera carteri</i>	<i>Helicosphaera sellii</i>	<i>Gephyrocapsa oceanica</i> s.l.	<i>Gephyrocapsa</i> sp. 3	<i>Gephyrocapsa</i> small	<i>Gephyrocapsa</i> large	<i>Coccolithus pelagicus</i>
CN15	167-1015A-1H-CC	7	G	A	A		P		C		A	C/F	
CN15	2H-CC	16.5	G/M	R	P		R		R		C		
CN15	3H-CC	26	G	RR	P				P		P		
	4H-CC	35.5	P/M	RR					RR				R
CN15	5H-CC	45	M/G	F	P				P		P		
CN15	6H-CC	54	G	R	P				P		P		
CN15	7H-CC	64	M/G	RR	P		P				P		
CN15	8H-CC	73.5	M	F	C		P				C		
CN15	9H-top		M/G	F	C				P		C		
CN15	9H-CC	83	G	C	C				P		C		
	10H-CC	92.5	P	RR					P				
CN15	11H-CC	102	M/G	F/C	P				P		P		
CN15	12H-CC	111.5	G	F	P				P		P		
CN15	13H-CC	121	G	RR	P								
CN15	14H-CC	130.5	P	RR	P				P				
CN15	15H-CC	140	G	A	C		R		P		A	C	
CN15	16H-CC	149.5	G	R	P				P				
	167-1015B-												
CN15	1H-CC	2.3	G	F/C	C		R			P	C		
CN15	2H-CC	11.8	G	A	A		R		C	P	C		
CN15	3H-CC	21.3	M	R	P		P		P				
CN15	4H-CC	30.8	P	RR	P				P				
	5H-CC	40.3		B									
CN15	6H-CC	49.8	G	RR	P		P		R		F		
CN15	7H-CC	59.3	M/G	A	A		P		C		C		
	8H-CC	68.8		B									
	9H-CC	78.3		B									
CN15	10H-CC	87.8	G	C	C		R		P		C		
CN15	11H-CC	99.3	P/M	RR	P				P				
CN15	12H-CC	106.8	G	C	C						C	C	

Note: See "Explanatory Notes" chapter for abbreviations.

Table 5. Distribution and abundances of diatoms in Holes 1015A and 1015B.

Core, section, interval	Depth (mbsf)	Abundance	Preservation	<i>Coccinodiscus marginatus</i>	<i>Coccinodiscus radiatus</i>	<i>Denticulopsis</i> cf. <i>Ayalina</i>	<i>Denticulopsis lauta</i> s.l.	<i>Rhizosolenia barboi</i>	<i>Thalassionema nitrschioides</i>	<i>Thalassiosira</i> sp.	Diatom fragments (girdle bands)			Diatom fragments	Sponge spicules
											P	C	R		
167-1015A-1H-CC	7.0	T	P		P				P	P	C			R	
2H-CC	16.5	T	P			P			P	P				R	
3H-CC	26.0	T	P	P				P							
4H-CC	35.5	B													
5H-CC	45.0	T	P	P										P	
6H-CC	56.0	T	P											P	P
7H-CC	64.0	B													
8H-CC	73.5	T	P	P											
9H-CC	83.0	T	P											P	P
10H-CC	92.5	B													T
11H-CC	102.0	B													T
12H-CC	111.5	B													T
13H-CC	121.0	B													T
14H-CC	130.5	B													T
15H-CC	140.0	B													T
16H-CC	149.5	B													P
167-1015B-1H-CC	2.3	T	P								F	R	R		
2H-CC	11.8	T	P			T						T	F		
3H-CC	21.3	B													
4H-CC	30.8	B													
5H-CC	40.3	B													
6H-CC	49.8	B													T
7H-CC	59.3	B													T
8H-CC	68.8	B													
9H-CC	78.3	B													
10H-CC	87.8	T	P			P								P	P
11H-CC	97.3	B													
12H-CC	106.8	T	P							P					T

Notes: P = present; more detailed abundance information not available. See "Explanatory Notes" chapter for other abbreviations.

Table 6. Site 1015 composite depth section.

Core, section	Offset (m)	Depth	
		(mbsf)	(mcd)
167-1015A-			
1H-1	0.00	0.00	0.00
2H-1	0.58	7.00	7.58
3H-1	0.99	16.50	17.49
4H-1	1.98	26.00	27.98
5H-1	1.98	35.50	37.48
6H-1	1.98	45.00	46.98
7H-1	1.98	54.50	56.48
9H-1	1.98	73.50	75.48
10H-1	1.98	83.00	84.98
12H-1	1.98	102.00	103.98
14H-1	1.98	121.00	122.98
15H-1	1.98	130.50	132.48
16H-2	1.98	140.92	142.90
167-1015B-			
1H-1	0.00	0.00	0.00
2H-1	-0.05	2.30	2.25
3H-1	1.33	11.80	13.13
4H-1	2.48	21.30	23.78
5H-2	2.48	31.43	33.91
6H-1	2.48	40.30	42.78
7H-1	2.01	49.80	51.81
8H-1	2.01	59.30	61.31
9H-1	2.01	68.80	70.81
10H-1	-3.63	78.30	74.67
11H-1	-3.63	87.80	84.17

Note: This table is also on CD-ROM, back pocket, this volume.

cause the thicker sandy turbidite sequences were too disturbed by drilling or not recovered at all.

Following construction of the composite depth section for Site 1015, a single spliced record was assembled from the aligned cores down to 36 mcd. Hole 1015A was used as the backbone of the sampling splice. Hole 1015B was used to splice across core gaps in Hole 1015A. The composite depths were aligned so that tie points between adjacent holes occurred at exactly the same depths in meters composite depth. Intervals having significant disturbance or distortion were avoided if possible. The Site 1015 splice (Table 7, also on CD-ROM, back pocket) can be used as a sampling guide to recover a single continuous sedimentary sequence between 0 and 36 mcd.

INORGANIC GEOCHEMISTRY

We collected nine interstitial water samples from Hole 1015A at depths ranging from 4.45 to 134.90 mbsf. Although the chemical composition of interstitial waters at this site (Table 8) indicates that organic matter diagenesis, biogenic opal dissolution, and authigenic mineral precipitation and/or ion exchange reactions are significant influences, the nature of the sediments and the effects of drilling and recovery on them make it problematic to distinguish primary geochemical signals from contamination by seawater drilling fluid.

Chlorinity increases from 541 mM at 4.45 mbsf to ≥ 550 mM from 39.78 to 134.90 mbsf (Fig. 7). Salinity, measured refractively as total dissolved solids, ranges from 31 to 33. Sodium concentrations by charge balance (Table 8) generally agreed within <5% with those

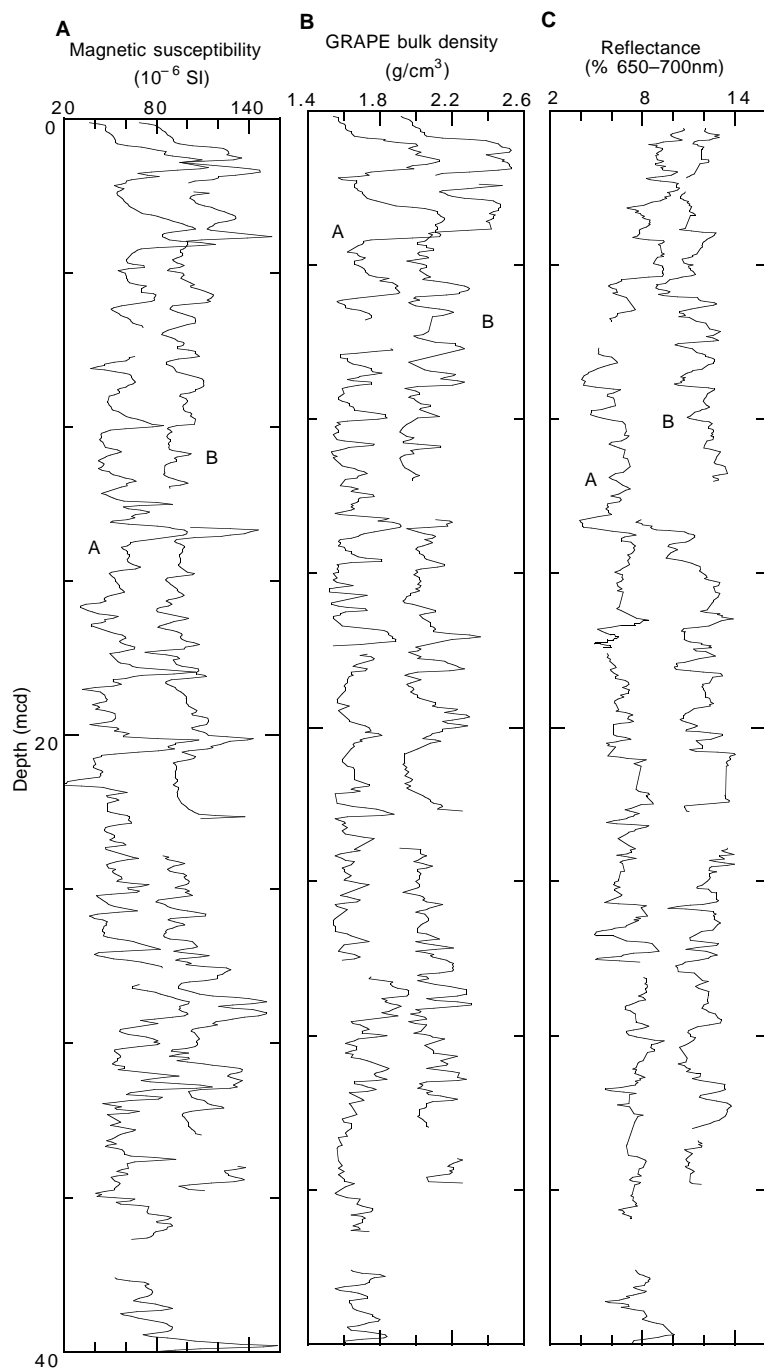


Figure 6. **A.** Smoothed (15-cm Gaussian) magnetic susceptibility data for the upper 36 m from Site 1015 on the mcd scale. Holes 1015A and 1015B are offset from each other by a constant (40×10^{-6} SI). **B.** Smoothed (15-cm Gaussian) GRAPE bulk density data for the upper 36 m from Site 1015 on the mcd scale. Holes 1015A and 1015B are offset from each other by a constant (0.4 g/cm^3). **C.** Smoothed (5-point running average) color reflectance (% 650–700 nm band) data for the upper 36 m from Site 1015 on the mcd scale. Holes 1015A and 1015B are offset from each other by a constant (5%).

Table 7. Site 1015 splice tie points.

Hole, core, section, interval (cm)	Depth			Hole, core, section, interval (cm)	Depth	
	(mbsf)	(mcd)			(mbsf)	(mcd)
1015A-1H-5, 12	6.12	6.12	tie to	1015B-2H-3, 87	6.17	6.12
1015B-2H-5, 7	8.44	8.39	tie to	1015A-2H-1, 81	7.81	8.39
1015A-2H-7, 22	16.22	16.8	tie to	1015B-3H-3, 67	15.47	16.8
1015B-3H-4, 52	16.82	18.15	tie to	1015A-3H-2, 27	17.16	18.15
1015A-3H-7, 117	25.56	26.55	tie to	1015B-4H-2, 127	24.07	26.55
1015B-4H-4, 92	26.72	29.2	tie to	1015A-4H-1, 122	27.22	29.2
1015A-4H-6, 97	34.38	36.36				

Note: This table is also on CD-ROM, back pocket, this volume.

Table 8. Interstitial water geochemical data, Hole 1015A.

Core, section, interval (cm)	Depth (mbsf)	pH	Alkalinity (mM)	Salinity	Cl ⁻ (mM)	Na ⁺ (mM)	SO ₄ ²⁻ (mM)	HPO ₄ ²⁻ (μM)	NH ₄ ⁺ (mM)	H ₄ SiO ₄ (μM)	Ca ²⁺ (mM)	Mg ²⁺ (mM)	Sr ²⁺ (μM)	Li ⁺ (μM)	K ⁺ (mM)
167-1015A-															
1H-3, 145-150	4.45	7.37	38.5	33.0	541	462	<0.7	101	2.7	595	5.96	48.0	98	13	9.8
2H-3, 145-150	11.45	7.38	31.8	32.5	546	466	<0.7	93	3.6	667	5.15	45.6	94	14	10.5
3H-3, 145-150	19.84	7.81	13.7	31.5	550	464	<0.7	15	4.3	355	3.88	40.7	89	14	10.1
4H-3, 140-150	30.40	7.42	11.3	31.0	547	461	<0.7	34	4.6	595	4.05	40.0	94	13	9.2
5H-3, 128-138	39.78	7.41	11.8	32.0	551	468	<0.7	26	6.9	493	3.99	38.5	94	13	9.5
6H-3, 124-134	49.24	7.50	13.7	32.0	551	467	<0.7	35	7.0	501	4.60	39.6	103	15	9.7
9H-3, 135-145	77.22	7.56	ND	32.0	554		<0.7	17	6.2	438	4.13	35.9	94	15	9.9
12H-4, 127-137	106.84	7.66	16.8	32.0	550	478	<0.7	27	9.4	559	3.92	35.3	98	17	10.4
15H-3, 140-150	134.90	7.80	15.9	32.0	553	479	<0.7	17	7.7	491	4.55	35.3	103	19	10.0

Note: ND = value not determined.

measured by flame emission spectrophotometry were on average <4% higher than those estimated by charge balance (Table 8).

Alkalinity is >30 mM in the shallowest two samples from 4.45 to 11.45 mbsf, then decreases to values generally <15 mM at 19.84 mbsf and deeper (Fig. 7). The decline in alkalinity corresponds to increasingly sandy sediments in the interstitial water whole rounds and a drop in the "water yield" achieved by squeezing. Sulfate concentrations are below the detection limit (approximately 0.7 mM) in all samples. Phosphate concentrations are >90 μM in the two shallowest samples from 4.45 to 11.45 mbsf with high alkalinity, then decrease to <40 μM, with sample to sample variability. Ammonium concentrations increase with increasing depth to values as high as 9 mM at 106.84 mbsf. Like the phosphate profile, the ammonium profile shows sample to sample variability not consistent with simple diffusive control of these profiles, suggesting variable contamination by seawater drilling fluid.

Dissolved silicate concentrations range from 355 to 667 μM (Fig. 7). Strontium concentrations are slightly elevated over seawater values (Table 8).

Calcium concentrations decrease to 3.9 mM at 19.84 mbsf, then generally increase with increasing depth to values up to 4.6 mM in the deepest sample at 134.90 mbsf (Fig. 7). Magnesium concentrations generally decrease with increasing depth to values as low as 35 mM at 134.90 mbsf.

ORGANIC GEOCHEMISTRY

The organic geochemistry analyses performed at Site 1015 include measurements of volatile hydrocarbons, elemental composition, and Rock-Eval pyrolysis (for methods see "Organic Geochemistry" section, "Explanatory Notes" chapter, this volume).

Volatile Hydrocarbons

Because of shipboard safety and pollution prevention considerations, the concentrations of methane, ethane, propane, and higher molecular weight hydrocarbons were routinely monitored in Hole 1015A. The results are displayed in Figure 8 and Table 9. Headspace methane concentrations are high (5,429–44,236 ppm) throughout the entire core. No significant amounts of higher weight molecular hydrocarbons were observed, indicating that the methane was derived from biogenic degradation of organic matter, and thus is not significant for safety and pollution investigations. Whenever gas voids occurred, vacutainer samples were taken. Because of the direct gas sampling method, the methane concentrations of the vacutainer samples are higher than those of headspace samples. Methane/ethane ratios are high and show a gradual decrease from top to bottom of the hole.

Elemental Compositions

At Site 1015, 43 sediment samples were analyzed for total carbon, inorganic carbon, total nitrogen, and total sulfur. The results are presented in Table 10 (also on CD-ROM, back pocket, this volume) and Figure 9.

The percentage of calcium carbonate (CaCO₃) was calculated from the inorganic carbon concentrations by assuming that all carbonate occurs in the form of calcite. CaCO₃ concentrations are low (2.08–7.25 wt%) within the entire section. Turbidite sands generally show slightly lower CaCO₃ contents than turbidite silts and hemipe-

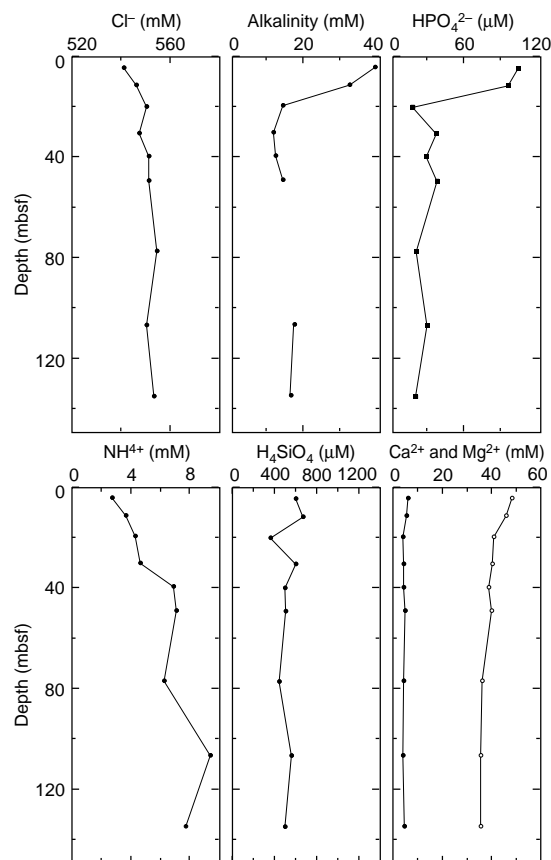


Figure 7. Interstitial water geochemical data, Site 1015. Solid circles = Ca, open circles = Mg.

lagic clays. This coincides with the occurrence of foraminifers and calcareous nannofossils (see “Biostratigraphy” section, this chapter).

Total organic carbon (TOC) content varies between 0.21 and 2.19 wt% (Table 10, also on CD-ROM, back pocket; Fig. 9). High TOC content of a turbidite sand (Sample 167-1015B-8H-4, 39–40 cm) is attributed to a high proportion of terrigenous organic matter, based on its high TOC/TN ratio (Table 10). Total nitrogen content varies between 0.06 and 0.28 wt%. Total sulfur content ranges from 0.10 to 0.80 wt% (Table 10).

Type of Organic Matter

In order to characterize the organic matter, TOC/TN ratio, Rock-Eval hydrogen index (HI), oxygen index (OI), and S_2/S_3 ratio were used. Results of Rock-Eval pyrolysis are shown in Table 11 and Figures 10 and 11. TOC/TN ratio of most samples range from 5 to 10 (Fig. 9), which indicates a predominant marine origin (Bordovskiy, 1965; Emerson and Hedges, 1988). In contrast, Rock-Eval pyrolysis shows that the selected samples are distributed in the region of Type III kerogen (Fig. 11), indicating that the organic matter was derived from higher plants such as land plants and/or seagrass (Tissot and Welte, 1984). These data are consistent with a microscopic observation of smear slides showing abundant plant debris (see “Lithostratigraphy” section, this chapter). The contradicting conclusions inferred from TOC/TN ratio and Rock-Eval pyrolysis likely result from the selective degradation of marine organic matter after deposition. If marine organic matter was incorporated into the sediment without severe degradation, because of the high sedimentation rates at this site, the TOC/TN ratio, which reflects mainly the initial composition of organic matter soon after deposition, shows a predominantly marine origin. On the other hand, terrigenous organic matter became predominant because of its selective preservation during early diagenesis. Therefore, Rock-Eval pyrolysis, which reflects the composition of organic matter after deposition, indicates a terrestrial origin. Further shore-based investigations such as the analyses of stable nitrogen isotopes, kerogens, and lipids may contribute to solving this problem.

PHYSICAL PROPERTIES

Multisensor Track Measurements

The shipboard physical properties program at Site 1015 included nondestructive measurements of bulk density, bulk magnetic susceptibility, P -wave velocity, and natural gamma-ray activity on whole sections of all cores using the MST. Magnetic susceptibility was measured at 5-cm intervals at low sensitivity (1-s measuring time) on all Site 1015 cores. Fluctuations in magnetic susceptibility are most likely associated with increases in the terrigenous input associated with the turbidites. For example, the high susceptibility values at about 55 mbsf (Fig. 12) occur where an abundance of amphibole was detected (see “Lithostratigraphy” section, this chapter).

GRAPE bulk density measurements were made at intervals of 5 cm. PWL velocity measurements were made at 20-cm intervals in Hole 1015A and at 5-cm intervals in Hole 1015B. Natural gamma-ray activity was measured with a 15-s count every 20 cm in Hole 1015B. The abrupt increase in velocity measured by the PWL from an average of 1580 to an average of 4020 m/s at about 5 mbsf is not the result of a significant change in lithology (see “Lithostratigraphy” section, this chapter) nor is it reflected in any associated changes in the whole-round wet-bulk density estimates from the GRAPE (Fig. 12). Rather, it is simply the arrival of the energy traveling around the core liner; the sediments were very gassy and attenuated energy traveling through the core.

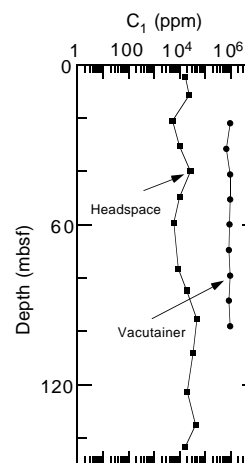


Figure 8. Concentrations of methane (C_1) obtained by the headspace and vacutainer techniques from Hole 1015B.

Table 9. Concentrations of methane (C_1) and ethane/ethene (C_2) obtained by the headspace and vacutainer techniques from Hole 1015A.

Core, section, interval (cm)	Depth (mbsf)	C_1 (ppm)	C_2 (ppm)	C_1/C_2
Headspace				
167-1015A-				
1H-4, 0-5	4.53	17,702		
2H-4, 0-5	11.53	24,969		
3H-4, 0-5	21.03	5,429		
4H-4, 0-5	30.53	10,332		
5H-4, 0-5	40.03	27,796		
6H-4, 0-5	49.53	10,079		
7H-4, 0-5	59.03	6,273		
9H-4, 0-5	78.03	9,388		
10H-2, 0-5	84.53	19,055		
11H-3, 0-5	95.53	47,298		
12H-5, 0-5	108.03	34,692		
14H-2, 0-5	122.53	20,865		
15H-4, 0-5	135.03	44,236		
16H-3, 0-5	143.03	17,081		
Vacutainer				
167-1015A-				
3H-4, 100-101	22.01	970,945	3	323,648
4H-4, 100-101	31.51	718,221	2	359,111
5H-4, 100-101	41.01	999,999	3	333,333
6H-4, 100-101	50.51	999,999	3	333,333
7H-4, 100-101	59.91	939,957	3	313,319
8H-4, 100-101	69.51	852,592	4	213,148
9H-4, 100-101	79.01	999,999	3	333,333
10H-4, 100-101	88.51	882,727	7	126,104
11H-4, 100-101	98.01	972,495	5	194,499

Index Properties

Discrete index properties, velocity, and thermal conductivity measurements were not made on the Site 1015 cores.

Color Reflectance

A 4-cm sampling interval was used for color reflectance measurements at Holes 1015A and 1015B. Large portions of both holes, however, were not measured because of gas voids and recurring turbidites. Reflectance is low at Site 1015, typically less than 10% within the visible bands (Fig. 13A). Spectral comparison of a sandy lithic turbidite and a laminated hemipelagic section shows only minor differences (Figs. 13B and 13C, respectively). Both spectra have a flat

Table 10. Depth variation in concentrations of inorganic carbon, calcium carbonate, total carbon, total organic carbon, total nitrogen, and total sulfur in weight percent (wt%) in Hole 1015B.

Core, section, interval (cm)	Depth (mbsf)	Inorganic carbon (wt%)	CaCO ₃ (wt%)	Total carbon (wt%)	Total organic carbon (wt%)	Total nitrogen (wt%)	Total organic carbon/total nitrogen	Total sulfur (wt%)
167-1015B-								
1H, 65-66	0.65	0.51	4.25	1.74	1.23	0.16	0.37	0.43
1H-2, 65-66	2.15	0.53	4.41	1.82	1.29	0.18	0.50	0.36
2H-2, 35-36	2.65	0.57	4.75	1.69	1.12	0.16	0.35	0.46
2H-2, 35-36	4.15	0.64	5.33	1.97	1.33	0.19	0.53	0.36
2H-3, 80-81	6.10	0.63	5.25	2.26	1.63	0.22	0.59	0.37
2H-4, 35-36	7.18	0.70	5.83	1.98	1.28	0.16	0.48	0.33
2H-5, 80-81	9.17	0.54	4.50	1.66	1.12	0.17	0.38	0.45
2H-6, 35-36	10.24	0.87	7.25	3.06	2.19	0.28	0.55	0.51
3H-1, 70-71	12.50	0.61	5.08	1.92	1.31	0.20	0.53	0.38
3H-2, 70-71	14.00	0.68	5.66	2.01	1.33	0.19	0.43	0.44
3H-3, 54-55	15.34	0.58	4.83	1.61	1.03	0.16	0.46	0.35
3H-4, 90-91	17.20	0.63	5.25	1.66	1.03	0.14	0.38	0.37
3H-5, 103-104	18.83	0.49	4.08	1.41	0.92	0.14	0.64	0.22
3H-6, 104-105	20.34	0.65	5.41	1.60	0.95	0.14	0.52	0.27
3H-7, 30-31	21.10	0.51	4.25	1.12	0.61	0.12	0.60	0.20
4H-1, 30-31	21.60	0.58	4.83	1.51	0.93	0.16	0.70	0.23
4H-3, 50-51	24.80	0.73	6.08	1.92	1.19	0.17	0.71	0.24
4H-4, 96-97	26.76	0.70	5.83	2.08	1.38	0.19	1.06	0.18
4H-5, 42-43	27.72	0.72	6.00	2.18	1.46	0.21	1.11	0.19
4H-6, 50-51	29.30	0.59	4.91	1.80	1.21	0.18	0.56	0.32
4H-7, 50-51	30.52	0.45	3.75	1.82	1.37	0.14	0.41	0.34
5H-1, 43-44	31.23	0.62	5.16	1.99	1.37	0.18	0.23	0.80
5H-2, 35-36	31.78	0.29	2.42	0.60	0.31	0.06	0.35	0.17
6H-1, 35-36	40.65	0.65	5.41	1.80	1.15	0.20	0.83	0.24
6H-2, 35-36	42.11	0.64	5.33	1.78	1.14	0.15	0.47	0.32
6H-3, 35-36	43.61	0.31	2.58	0.52	0.21	0.06	0.60	0.10
6H-4, 35-36	45.07	0.61	5.08	1.61	1.00	0.15	0.47	0.32
7H-1, 35-36	50.15	0.68	5.66	1.75	1.07	0.15	0.50	0.30
7H-2, 35-36	51.65	0.67	5.58	1.63	0.96	0.20	0.65	0.31
7H-3, 95-96	53.52	0.64	5.33	1.77	1.13	0.10	0.43	0.23
7H-4, 35-36	54.42	0.64	5.33	1.70	1.06	0.14	0.42	0.33
7H-5, 35-36	55.92	0.56	4.66	1.49	0.93	0.19	0.58	0.33
7H-6, 35-36	57.28	0.34	2.83	0.57	0.23	0.04	0.44	0.09
8H-2, 40-41	61.15	0.54	4.50	1.61	1.07	0.17	0.52	0.33
8H-3, 51-52	62.65	0.37	3.08	1.21	0.84	0.11	0.39	0.28
8H-4, 39-40	63.93	0.50	4.17	2.45	1.95	0.11	0.18	0.62
9H-1, 5-6	68.85	0.25	2.08	1.17	0.92	0.09	0.26	0.34
9H-1, 50-51	69.30	0.63	5.25	1.51	0.88	0.23	0.96	0.24
9H-3, 6-7	71.86	0.57	4.75	1.52	0.95	0.12	0.41	0.29
10H-1, 18-19	78.48	0.54	4.50	1.60	1.06	0.14	0.74	0.19
10H-2, 60-61	79.59	0.76	6.33	1.77	1.01	0.22	1.16	0.19
10H-5, 24-25	83.58	0.70	5.83	1.83	1.13	0.21	0.78	0.27
11H-1, 29-30	88.09	0.64	5.33	1.91	1.27	0.15	0.68	0.22

Note: This table is also on CD-ROM, back pocket, this volume.

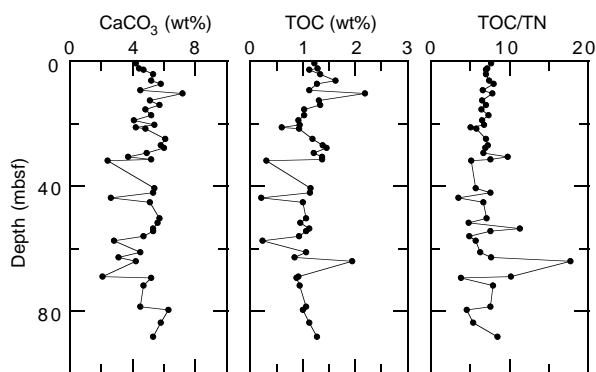


Figure 9. Depth variations of calcium carbonate (CaCO₃) and total organic carbon (TOC) contents and total organic carbon/total nitrogen (TOC/TN) ratio in sediments from Hole 1015B.

pattern between 400 and 950 nm; the average color reflectance is 5% for the turbidite and approximately 7% for the laminated hemipelagic interval. These low reflectance values and small differences in spectral shape are most likely because of the low biogenic calcium carbonate and opal content at Site 1015. The turbidites are barren or nearly barren of calcareous and siliceous microfossils, and the hemi-

pelagic sections are rich in terrigenous clay and contain less than 8% calcium carbonate (see “Organic Geochemistry” section, this chapter).

Digital Color Video

All cores from Site 1015 were imaged with the ODP color digital imaging system over 20-cm intervals to provide a 0.25-mm pixel. Digital color video data of CIELAB L* (see “Physical Properties” section, “Explanatory Notes” chapter, this volume) from Holes 1015A and 1015B show poor hole-to-hole correlation (Fig. 14).

SUMMARY

At Site 1015, in Santa Monica Basin of the California Borderland, we drilled to sample an upper Pleistocene sedimentary section in the hopes of obtaining a sedimentary section with similar resolution to Site 893 in the Santa Barbara Basin. Whereas high-resolution laminated intervals were found in the section, the sediments are ~85% turbidites (Fig. 15). Provided that radiocarbon age control can be achieved, however, the extremely fast sedimentation rate may allow reasonably detailed study of the transition from the last glacial maximum to the present. Because the basin sill depth is 740 mbsl, the sedimentary record was generated near the core of the modern oxygen minimum (Emery, 1960).

Table 11. Results of Rock-Eval pyrolysis for selected samples for Hole 1015B.

Core, section, interval (cm)	Depth (mbsf)	TOC (wt%)	T _{max} (°C)	S ₁ (mg/g)	S ₂ (mg/g)	S ₃ (mg/g)	PI (S ₁ /[S ₁ +S ₂])	S ₂ /S ₃	HI (100S ₂ /TOC)	OI (100S ₃ /TOC)
167-1015B-										
1H-1, 65-66	0.65	1.12	404	0.27	1.40	2.82	0.16	0.50	125	252
2H-3, 80-81	6.10	1.55	393	0.70	2.89	3.60	0.19	0.80	186	232
3H-2, 70-71	14.00	1.25	405	0.28	1.93	2.89	0.13	0.67	154	231
3H-7, 30-31	21.10	0.58	413	0.19	0.96	2.37	0.17	0.41	166	409
4H-6, 50-51	29.30	1.15	417	0.27	1.67	3.62	0.14	0.46	145	315
6H-1, 35-36	40.65	1.14	416	0.28	1.89	3.56	0.13	0.53	166	312
7H-5, 35-36	50.15	0.96	415	0.23	1.54	4.36	0.13	0.35	160	454
7H-5, 35-36	55.92	0.84	411	0.18	1.06	3.07	0.15	0.35	126	365
8H-3, 51-52	62.65	0.70	418	0.08	0.92	1.35	0.08	0.68	131	193
9H-1, 50-51	69.30	0.89	416	0.17	1.23	4.05	0.12	0.30	138	455
10H-2, 60-61	79.59	1.04	413	0.24	1.61	4.18	0.13	0.39	155	402
11H-1, 29-30	88.09	1.22	417	0.24	1.87	4.28	0.11	0.44	153	351

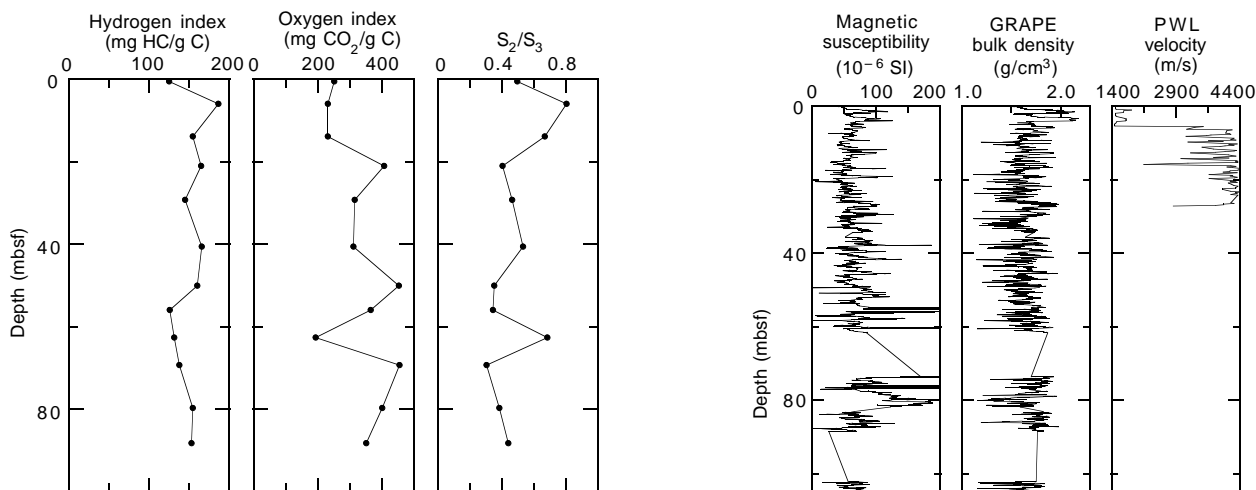
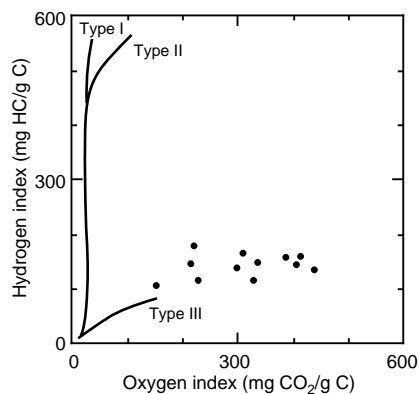
Figure 10. Depth variations of Rock-Eval hydrogen index (HI), oxygen index (OI), and S₂/S₃ ratio in sediments from Hole 1015B.

Figure 11. A "van Krevelen" type diagram (HI-OI diagram) for selected samples from Hole 1015B. Types I and II originate mainly from aquatic organisms, whereas Type III originates from oxidized marine organic matter and land plants (Tissot and Welte, 1984).

Site 1015 was double cored to a depth of 98 mbsf and single cored to 150 mbsf. A continuous sedimentary sequence could only be generated to 34 mbsf because of flow-in associated with certain large turbidites. The base of the sediment column is very young, less than 85 ka by calcareous nannofossil biostratigraphy, giving this site almost twice the sedimentation rate of Site 893 in the Santa Barbara Basin.

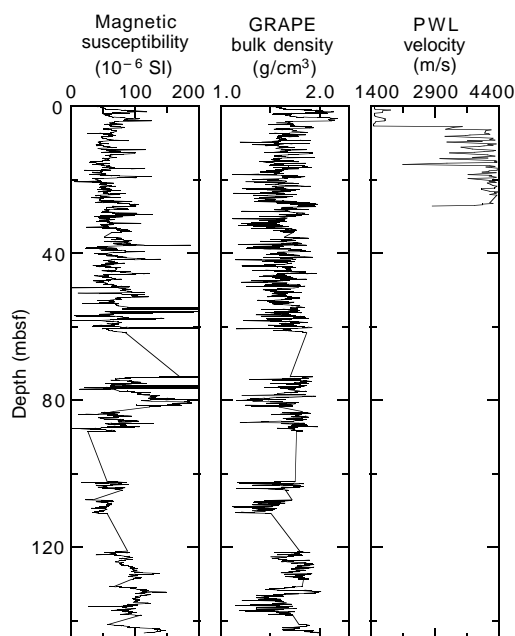


Figure 12. MST data from Hole 1015A.

REFERENCES

- Behl, R.J., and Kennett, J.P., 1996. Brief interstadial events in Santa Barbara basin, NE Pacific, during the past 60 kyr. *Nature*, 379:243-246.
- Bordovskiy, O.K., 1965. Accumulation and transformation of organic substances in marine sediment, 2. Sources of organic matter in marine basins. *Mar. Geol.*, 3:5-31.
- Drake, D.E., Kolpack, R.L., and Fischer, P.J., 1972. Sediment transport on the Santa Barbara-Oxnard Shelf, Santa Barbara Channel, California. In Swift, D.J.P., Duane, D.B., and Pilkey, O.H. (Eds.), *Shelf Sediment Transport: Process and Pattern*: Stroudsburg, PA (Dowden, Hutchinson, and Ross), 307-331.
- Emerson, S., and Hedges, J.I., 1988. Processes controlling the organic carbon content of open ocean sediments. *Paleoceanography*, 3:621-634.
- Emery, K.O., 1960. *The Sea Off Southern California: A Modern Habitat of Petroleum*: New York (Wiley).
- Kennett, J.P., Baldauf, J.G., and Lyle, M. (Eds.), 1995. *Proc. ODP, Sci. Results*, 146 (Pt. 2): College Station, TX (Ocean Drilling Program).
- Kennett, J.P., and Venz, K., 1995. Late Quaternary climatically related planktonic foraminiferal assemblage changes: Hole 893A, Santa Barbara Basin, California. In Kennett, J.P., Baldauf, J.G., and Lyle, M. (Eds.), *Proc. ODP, Sci. Results*, 146 (Pt. 2): College Station, TX (Ocean Drilling Program), 281-293.
- Lyle, M., Galloway, P.J., Liberty, L.M., Mix, A., Stott, L., Hammond, D., Gardner, J., Dean, W., and the EW9504 Scientific Party, 1995a. Data sub-

mission. W9406 and EW9504 site surveys of the California margin proposed drillsites, Leg 167 (Vol. 1): Site maps and descriptions. Boise State Univ., *CGISS Tech. Rep.*, 95–11.

———, 1995b. Data submission. W9406 and EW9504 site surveys of the California margin proposed drillsites, Leg 167 (Vol. 2): Seismic profiles. Boise State Univ., *CGISS Tech. Rep.*, 95–12.

Savrda, C.E., Bottjer, D.J., and Gorsline, D.S., 1984. Development of a comprehensive oxygen-deficient marine biofacies model: evidence from Santa Monica, San Pedro and Santa Barbara basins, California Continental Borderland. *AAPG Bull.*, 68:1179–1192.

Stow, D.A.V., and Wetzel, A., 1990. Hemiturbidite: a new type of deep-water sediment. In Cochran, J.R., Stow, D.A.V., et al., *Proc. ODP, Sci. Results*, 116: College Station, TX (Ocean Drilling Program), 25–34.

Tissot, B.P., and Welte, D.H., 1984. *Petroleum Formation and Occurrence* (2nd ed.): Heidelberg (Springer-Verlag).

Ms 167IR-109

NOTE: For all sites drilled, core-description forms (“barrel sheets”) and core photographs can be found in Section 3, beginning on page 499. Smear-slide data can be found in Section 4, beginning on page 1327. See Table of Contents for material contained on CD-ROM.

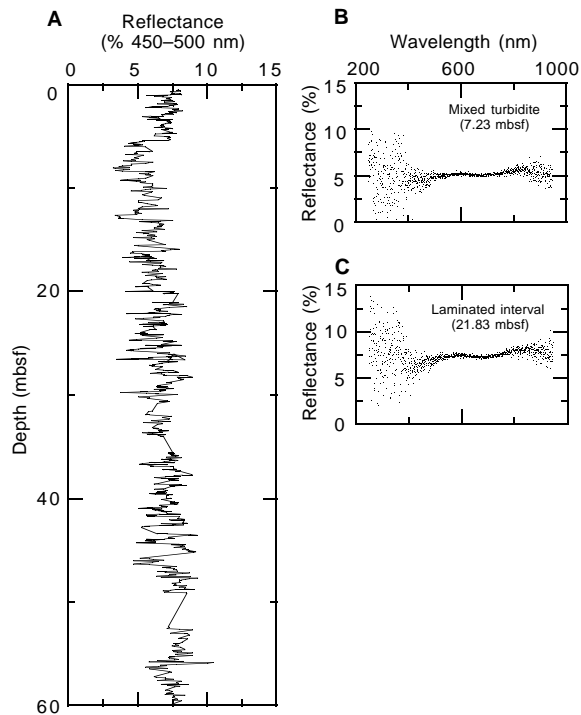


Figure 13. Summary of color reflectance data at Hole 1015A. **A.** Percent color reflectance of the 450–500-nm band average from 0 to 60 mbsf. **B.** Characteristic spectra of a turbidite. **C.** Characteristic spectra of a laminated interval.

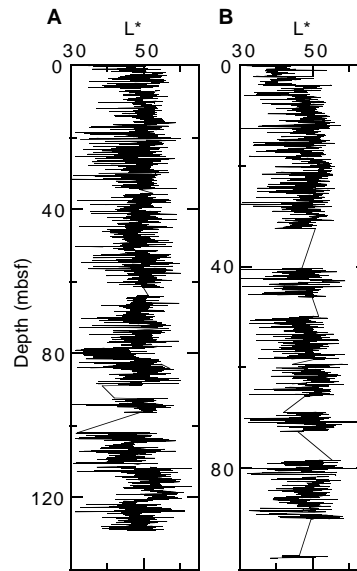


Figure 14. Intensity of color CIELAB L* from the digital color video for Holes 1015A (A) and 1015B (B). Data were decimated at 2-cm intervals.

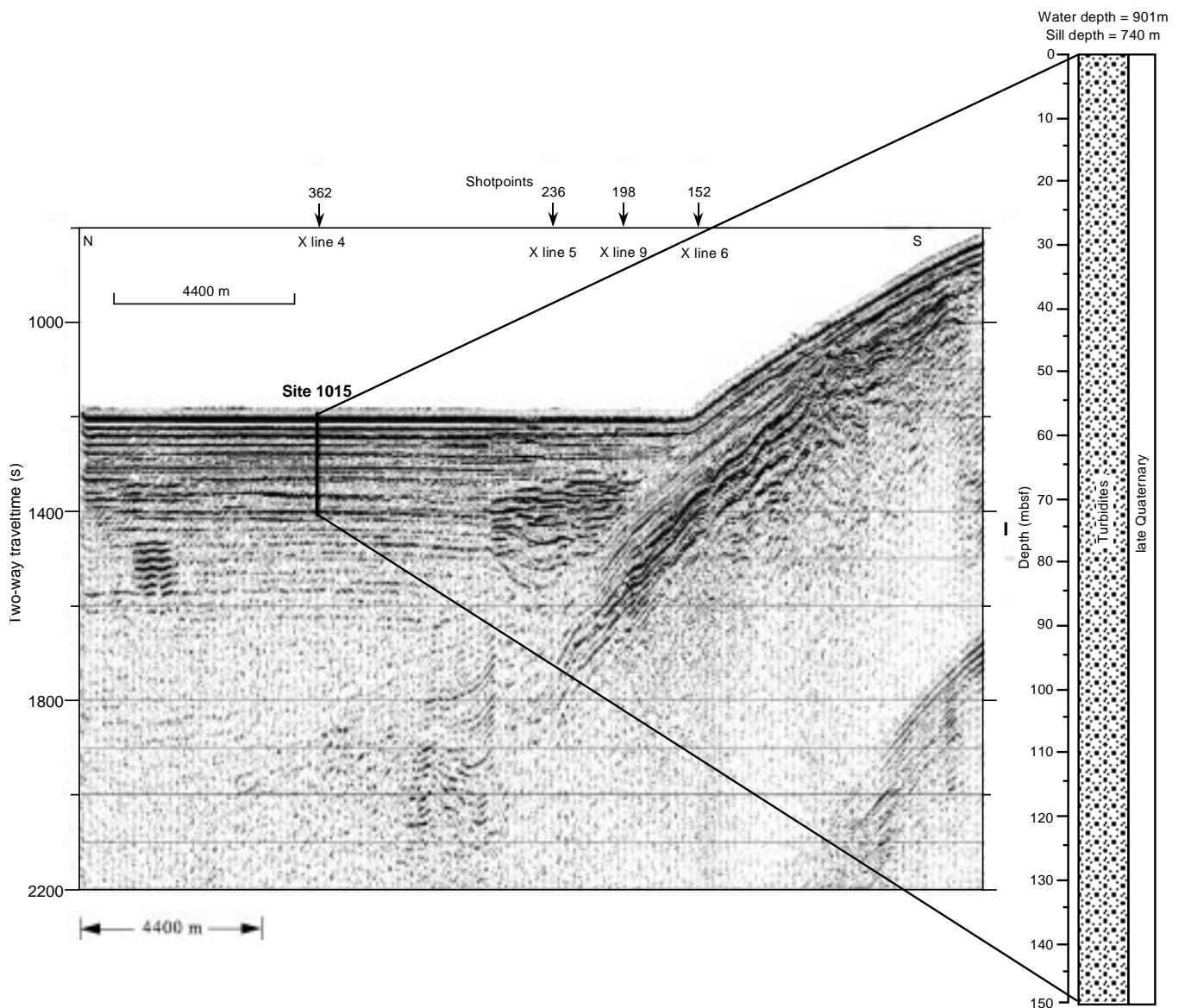


Figure 15. Comparison of the lithostratigraphic column at Site 1015 and a seismic profile through the site (Line EW9504 BA4-1; Lyle et al., 1995a, 1995b). Ties are calculated assuming 1600 m/s seismic velocity in the sediments. On y-axis, (s) = milliseconds.